Crossing of Shears Bands in ^{197}Pb: $B(M1)$ Values and Semiclassical Description

J. R. Cooper,[1] R. Krücken,[1] C. W. Beausang,[1] J. R. Novak,[1] A. Dewald,[2] T. Klug,[2] G. Kemper,[2] P. von Brentano,[2] M. P. Carpenter,[3] R. V. F. Janssens,[3] C. J. Lister,[3] and I. Wiedenhöver[3,*]

[1]*A. W. Wright Nuclear Structure Laboratory, Yale University, New Haven, Connecticut 06520*

[2]*Institut für Kernphysik, Universität zu Köln, Köln, Germany*

[3]*Argonne National Laboratory, Argonne, Illinois 60439*

(Received 25 April 2001; published 5 September 2001)

Subpicosecond lifetimes of states in shears band 1 in ^{197}Pb were measured by means of the recoil distance method employing Gammasphere and the New Yale Plunger Device. The extracted reduced matrix elements, $B(M1)$, show a clear sensitivity to the crossing of different shears configurations reflecting the closing and reopening of the shears blades. The energies and $B(M1)$ values in the band crossing region are successfully described in the framework of the semiclassical model of the shears bands. The relevance of core rotation contributions are shown. The results point to the existence of shears states with an angular momentum coupling angle larger than 90°.

DOI: 10.1103/PhysRevLett.87.132503 PACS numbers: 27.80.+w, 21.10.Ky, 21.10.Re, 23.20.–g

The so-called shears mechanism seems experimentally well established as the mechanism governing the magnetic dipole ($M1$) bands in the neutron-deficient Pb isotopes [1–4]. In particular, recent lifetime measurements [5–8] have unambiguously shown that the reduced transition matrix elements $B(M1)$ characteristically decrease with increasing angular momentum. Experimental $B(M1)$ values and transition energies closely follow predictions of the tilted-axis-cranking (TAC) [9] model, which provides a microscopic interpretation of the dipole bands.

The underlying configuration of the shears bands is based on the perpendicular coupling of the angular momenta of high-j, high-K proton particles and high-j, low-K neutron holes. This coupling scheme was confirmed by the results of a recent g-factor measurement in ^{193}Pb [10]. With increasing angular momentum the quasiparticle angular momenta j_π, j_ν align gradually with the total angular momentum vector J. This motion resembles the closing of the blades of a pair of shears, lending the name "shears bands" to the observed bands [4].

In order to describe the rotational-like behavior of these bands it was suggested that the spherical symmetry of the system is broken by the anisotropic current distribution of the orbital motion of the high-j quasiparticles. An orientation of the system can be defined and rotational motion can occur. The large magnetic dipole component perpendicular to the total angular momentum can be viewed as rotating around J, and this rotating magnetic dipole induces enhanced $M1$ transitions. This motion has been named "magnetic rotation" [11] as opposed to the more familiar "electric rotation" of a quadrupole deformed charge density leading to rotational bands with enhanced electric quadrupole ($E2$) transitions. In another approach the rotational-like pattern can be explained in terms of the interaction of the quadrupole moments of the quasiparticle configurations with the quadrupole vibrational field of the core, which leads to a parabolic spin dependence of the level energies [12–15].

A remarkable result of the previous investigation of ^{197}Pb was the observed rise in the $B(M1)$ values of shears band 1 in ^{197}Pb (the band is labeled according to Ref. [16]) at the point of a small up bend in the spin vs rotational frequency plot [6]. At the same time band 2 in ^{197}Pb, which does not exhibit an up bend, showed the usual decrease in $B(M1)$ values associated with the shears mechanism. It was speculated that the rise of $B(M1)$ values in band 1 may reflect the reopening of the shears blades due to a band crossing [1,6]. Clark and Macchiavelli [1] provided a schematic prediction of the behavior of the $B(M1)$ values due to the crossing of the different shears configurations.

In this Letter we report on results from a subpicosecond lifetime measurement on states in shears band 1 of ^{197}Pb [16–19] that for the first time reveal the details of the band crossing of different shears configurations. After presenting the experimental procedure and data analysis, band-mixing calculations are presented that are based on the description of the shears configurations by a semiclassical approach [14,15,20].

Excited states in ^{197}Pb were populated in the reaction ^{176}Yb(^{26}Mg, $5n$)^{197}Pb at a beam energy of 130 MeV. The beam was delivered by the ATLAS accelerator of Argonne National Laboratory. The γ rays emitted by the excited ^{197}Pb nuclei were detected by the Gammasphere array [21]. The 1 mg/cm^2 thick ^{176}Yb target foil was supported by a 1.5 mg/cm^2 Ta layer that faced the incoming beam. The recoiling nuclei left the target with a velocity of $v = 0.01c$ and were stopped in a 5 mg/cm^2 thick Au stopper foil. Target and stopper foil were mounted inside the New Yale Plunger Device (NYPD) [22]. An average of 150×10^8 events with at least four Compton suppressed gamma-ray energies were collected at each of ten distances [1, 2, 3, 4.5, 6.5, 9, 12, 16, 22, and 32 μm, with respect to the electrical contact of the foils]. The separation of the foils was kept constant to within a few percent by a feedback system [23] that relies on the capacitance between the foil and distance corrections by a piezoelectric

crystal. This stabilization is crucial since the uncertainty of the distance difference enters into the uncertainties of the lifetimes.

For each distance separate background-subtracted, double-gated spectra were sorted for each level of interest in the band and each of the Gammasphere detector rings at 35° (combination of detectors positioned at 32° and 37°), 54° (50° and 58°), 126° (combination of 122° and 130°), 146° (143° and 148°), and 163°. Figure 1 shows sample spectra. Intensities of the unshifted and Doppler-shifted components were extracted for the depopulating and populating transitions of each of these levels. The gating conditions required coincidences with higher lying transitions, thus selecting the decay path of the nuclei and eliminating any contributions of side feeding in the lifetime analysis.

Lifetimes for the levels of interest were extracted using the differential decay curve method (DDCM) [24,25]. All of the measured lifetimes are in the range from 0.5 to 1.1 ps indicating the difficulty of the present experiment. [The recoil distance method (RDM) is commonly used to measure lifetimes above 1 ps.] The measurement of such short lifetimes was possible only due to the effective population times of the levels of interest, on the order of 2 ps. Because of the short lifetimes one can no longer make the usual assumption that the slowing down time in the stopper foil can be neglected [26]. Correction factors were calculated, as suggested by Dewald [26], which vary smoothly from 50% at 0.5 ps to 30% at 1.1 ps. Table I summarizes the lifetimes and $B(M1)$ values obtained in this experiment. The $B(M1)$ values are shown as a function of level spin in Fig. 2.

The $B(M1)$ values first fall with increasing spin as expected for a shears configuration but rise in the spin region of the first band crossing. The increase of the $B(M1)$ values in the first band crossing region lends support to the large $B(M1)$ values found above this first crossing in the DSAM experiment of Ref. [6].

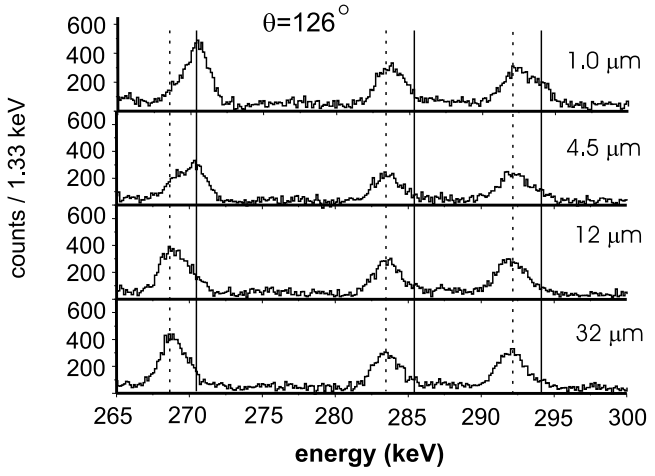

FIG. 1. Gated spectra for the detector ring at 126° at distances of 1.0, 4.5, 12, and 32 μm. The positions of shifted (dashed line) and unshifted (solid line) components are indicated for the $\frac{31^-}{2} \rightarrow \frac{29^-}{2}$ (270.5 keV), $\frac{41^-}{2} \rightarrow \frac{39^-}{2}$ (293.8 keV), and $\frac{47^-}{2} \rightarrow \frac{45^-}{2}$ (285.2 keV) transitions.

In order to understand the experimental $B(M1)$ values we employ a semiclassical model [14,15,20] in which the shears bands result from the simple recoupling of the angular momentum vectors generated by the proton-particle and neutron-hole configuration, respectively. The quasiparticle angular momenta j_π and j_ν are coupled by the shears angle θ to the total angular momentum J (see inset of Fig. 2). The interaction leading to the closing of the shears blades can be described by a simple quadrupole-quadrupole interaction, which may originate from the interaction of the quadrupole moment of the quasiparticle configurations with the vibrational field of the core [12,13,15]. Thus, the energy states for the unperturbed shears configuration are given by

$$E(J) = E_0 + V_2 P_2[\cos(\theta)], \tag{1}$$

with

$$\cos(\theta) = \frac{J(J+1) - j_\nu(j_\nu+1) - j_\pi(j_\pi+1)}{2\sqrt{j_\nu(j_\nu+1)j_\pi(j_\pi+1)}}. \tag{2}$$

We use the quasiparticle configurations $A11$ $[\pi(i_{13/2}h_{9/2})_{11} \otimes \nu(i^{-1}_{13/2})]$, $ABC11$ $[\pi(i_{13/2}h_{9/2})_{11} \otimes \nu(i^{-3}_{13/2})_{33/2}]$, and $ABCEF11$ $\{\pi(i_{13/2}h_{9/2})_{11} \otimes \nu[i^{-3}_{13/2} \times (f_{5/2}p_{3/2})]_{39/2}\}$ [16,19] as unperturbed configurations. For each configuration V_2 is calculated as nV_0, with n being the number of quasiparticles involved in the shears, e.g., $n = 3$ for the A11 configuration. A value of $V_0 = 0.48$ MeV, which is well within the range deduced in Ref. [15], was found to best reproduce the data. A three band mixing calculation was performed, in which the values of E_0 and the interaction between the bands were fitted to reproduce the energies of the experimentally

TABLE I. Mean level lifetimes τ and reduced matrix elements $B(M1)$ for the states in shears band 1 of ^{197}Pb from the present work. The corrected lifetimes $\tau_{\rm corr}$ were calculated from the uncorrected $\tau_{\rm uncorr}$ according to [26] to account for the effects of the slowing process in the stopper foil.

Spin$^\pi$ ($\hbar$)	E_γ (keV)	$\tau_{\rm uncorr}$ (ps)	$\tau_{\rm corr}$ (ps)	$B(M1)$ (μ_N^2)
$\frac{29}{2}^-$	152.6	0.8 (2)	1.1 (3)	3.8 (9)
$\frac{31}{2}^-$	270.5	0.47 (12)	0.71 (19)	2.5 (4)
$\frac{33}{2}^-$	359.1	0.39 (10)	0.60 (16)	1.6 (3)
$\frac{35}{2}^-$	369.8	0.29 (8)	0.49 (15)	1.8 (4)
$\frac{37}{2}^-$	385.0	0.8 (4)	1.0 (5)	0.8 (4)
$\frac{39}{2}^-$	365.2	0.6 (3)	0.8 (4)	1.1 (4)
$\frac{41}{2}^-$	293.8	0.47 (14)	0.7 (2)	2.1 (5)
$\frac{43}{2}^-$	227.6	0.52 (17)	0.8 (3)	3.1 (12)

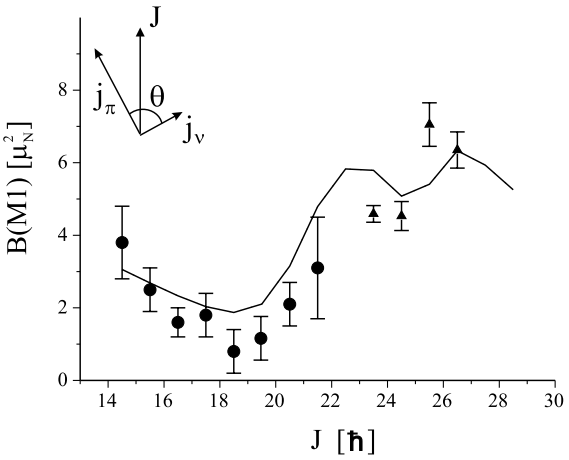

FIG. 2. $B(M1)$ values as a function of level spin for shears band 1 in ^{197}Pb. The results of this work (filled circles) and a previous DSAM experiment [6] (filled triangles) are compared to the results of our band-mixing calculations (solid line) using the semiclassical model [14,15,20]. As an inset the coupling of proton and neutron quasiparticle angular momenta to the total angular momentum J is shown.

observed band. The reasonable agreement between the experimental energies and the results of the mixing calculations can be seen in Fig. 3. Interactions of 0.7 and 0.1 MeV were used for the mixing of configurations $A11/ABC11$ and $ABC11/ABCEF11$, respectively. The interaction of 0.7 MeV seems rather large but does provide the best fit of the experimental energies using the parametrization of the unperturbed bands.

At this point we would like to remark that within the present model it is impossible to describe the crossing between the $A11$ and $ABC11$ configurations without the introduction of a small amount of rotational angular momentum from the core. This is apparent when one considers that the $A11$ configuration can only generate a

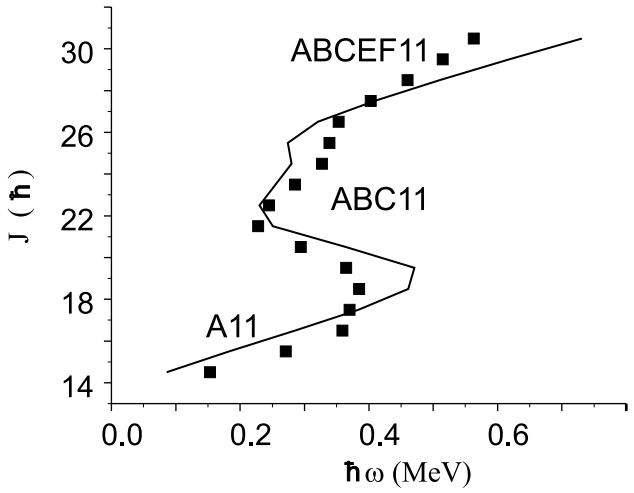

FIG. 3. Experimental (filled squares) and calcualted (solid line) angular momentum vs rotational frequency (gamma-ray energy) for shears band 1 in ^{197}Pb.

total angular momentum of 17.5 $\hbar$ while mixing between the $A11$ and $ABC11$ configuration occurs up to a spin of 21.5 $\hbar$. The difference in angular momentum has to come from the core rotation. Therefore, we have included the core rotation [20] into our calculations, which leads to a modification of Eq. (1) to

$$E(J) = E_0 + R^2/2\Im_{\text{core}} + V_2 P_2[\cos(\theta)]. \quad (3)$$

Here R is the core angular momentum along the total angular momentum vector and $\Im_{\text{core}}$ is the core moment of inertia. The value of $\Im_{\text{core}} = 3\hbar^2/\text{MeV}$ was extracted from energy fits to shears bands from ^{193}Pb to ^{199}Pb.

The decomposition of our mixing calculations is summarized in Fig. 4. In the bottom panel of Fig. 4 the contributions of the core angular momentum are plotted as a function of the total angular momentum. One can see that near the band head of the $A11$ configuration core rotation does not play a role, while a contribution of about 4 $\hbar$ is needed at spin 21.5 $\hbar$. Generally, the contribution of the core rotation increases almost linearly with spin for each configuration [20]. This is in general agreement with the results of TAC calculations, which are discussed in Ref. [16]. It is interesting to note that one actually needs a negative spin contribution of the core rotation near the band head in order to successfully describe the lowest observed states for configuration $ABC11$.

Figure 4 also shows the squared mixing amplitudes of the three unperturbed configurations in the wavefunctions of the observed states (top) as well as the opening angle of the unperturbed shears configurations (middle) as a function of the total angular momentum. One can see that the

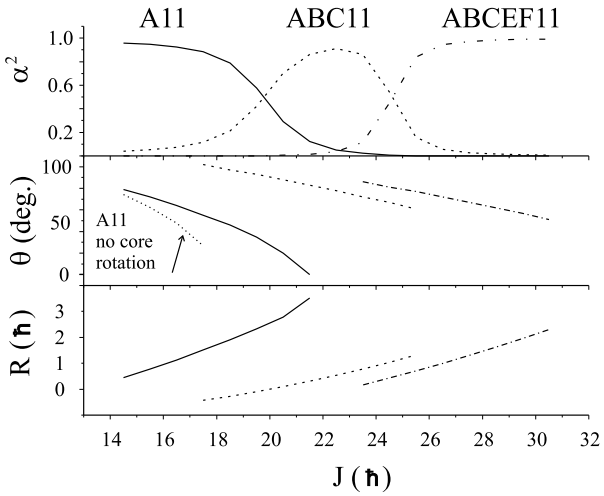

FIG. 4. Top: Squared mixing amplitudes α^2 of the shears configurations $A11$ (solid line), $ABC11$ (dashed line), and $ABCEF11$ (dash-dotted line) as a function of the total angular momentum J. *Middle:* Opening angle θ for each shears configuration as a function of J including the core contributions R to J. Also shown is the opening angle of configuration $A11$ (dotted line) if no core rotation is included. *Bottom:* Contribution of the core rotational angular momentum R to the total angular momentum for each shears configuration.

$A11$ configuration (including core rotation) terminates at spin 21.5 $\hbar$. In the middle panel we have also indicated the opening angle for the $A11$ configuration if no core rotation were included in order to stress its importance for a correct description of the bands. It is notable that for configuration $ABC11$ we require opening angles $\theta > 90°$ at the lowest angular momenta.

$B(M1)$ values for each transition were calculated using the relationship [14]

$$B(M1) = \frac{3}{4\pi}\,\mu_{\perp}^2 = \frac{3}{8\pi}\,g_{\rm eff}^2 j_{\pi}^2 \sin\theta_{\pi}\,. \qquad (4)$$

The calculated $B(M1)$ values for band 1 in ^{197}Pb are shown in Fig. 2 in comparison to the data. A value of $g_{\rm eff} = 0.9$ was used for the effective g factor of all three configurations. This value best reproduced the data and is close to the value of $g_{\rm eff} = 0.92$ shown to reproduce on average the $B(M1)$ values in the Pb region [14]. The agreement of the three band mixing calculations and the experimental data is remarkable.

In summary, we have measured subpicosecond lifetimes of states in shears band 1 of ^{197}Pb using the recoil distance method. The experiment was performed using the NYPD in conjunction with Gammasphere. The absolute $B(M1)$ values deduced from the lifetimes show a characteristic pattern that reflects the crossing of the $A11$ and $ABC11$ configurations. At higher spins the $ABC11$ configuration is crossed by the $ABCEF11$ configuration where the $B(M1)$ values from a previous DSAM experiment show a characteristic rise. The $B(M1)$ values indicate that with increasing spin the blades of the $A11$ configuration close. At the crossing point a mixing occurs between an almost closed $A11$ shears configuration and the $ABC11$ configuration with a coupling angle of larger than 90° at the band head, leading to a jump in the $B(M1)$ values. The crossing of the $ABC11$ and $ABCEF11$ configurations does not occur as close to the termination point and band head of the respective configurations. Thus the change in $B(M1)$ values is not quite as dramatic.

We have shown that the semiclassical model by Macchiavelli *et al.* [14,15,20] provides an excellent quantitative description of the energies and $B(M1)$ values if a certain amount of core rotation is included. Our results show the relevance of core rotation contributions and suggest the existence of states with shears angles larger than 90°.

Finally, we would like to point to the possibility to use the shears bands to study in detail the particle-core coupling mechanism [12,13]. We hope our article will encourage such work as well as more detailed theoretical predictions of the strength of this coupling.

We would like to acknowledge significant contributions by R. M. Clark and A. O. Macchiavelli. This work was funded in part by the U.S. DOE under Grant No. DE-FG02-91ER-40609 and Contract No. W-31-109-ENG-38 as well as the German Federal Minister for Education and Research (BMBF) under Contract No. 06OK958.

*Present address:NSCL, Michigan State University, East Lansing, MI.

[1] R. M. Clark and A. O. Macchiavelli, Annu. Rev. Nucl. Part. Sci. **50**, 1 (2000).
[2] S. Frauendorf, Rev. Mod. Phys. **73**, 463 (2001).
[3] R. M. Clark *et al.,* Nucl. Phys. **A562**, 121 (1993), and references therein.
[4] G. Baldsiefen *et al.,* Nucl. Phys. **A574**, 521 (1994), and references therein.
[5] R. M. Clark *et al.,* Phys. Rev. Lett. **78**, 1868 (1997).
[6] R. M. Clark *et al.,* Phys. Lett. B **440**, 251 (1998).
[7] R. Krücken *et al.,* Phys. Rev. C **58**, R1876 (1998).
[8] G. Kemper *et al.,* Eur. Phys. J. **A11**, 121 (2001).
[9] S. Frauendorf, Nucl. Phys. **A557**, 259c (1993).
[10] S. Chmel *et al.,* Phys. Rev. Lett. **79**, 2002 (1997).
[11] S. Frauendorf, Z. Phys. A **358**, 163 (1997).
[12] V. Paar, Nucl. Phys. **A331**, 16 (1979).
[13] K. Heyde, P. van Isaker, M. Waroquier, J. L. Wood, and R. A. Meyer, Phys. Rep. **102**, 291 (1983).
[14] A. O. Macchiavelli *et al.,* Phys. Rev. C **57**, R1073 (1998).
[15] A. O. Macchiavelli *et al.,* Phys. Rev. C **58**, R621 (1998).
[16] A. Görgen *et al.,* Nucl. Phys. **A683**, 108 (2001).
[17] J. A. Becker *et al.,* Nucl. Instrum. Methods Phys. Res., Sect. B **79**, 313 (1993).
[18] J. R. Hughes *et al.,* Phys. Rev. C **48**, R2135 (1993).
[19] G. Baldsiefen *et al.,* Nucl. Phys. **A587**, 562 (1995).
[20] A. O. Macchiavelli *et al.,* Phys. Lett. B **450**, 1 (1999).
[21] I. Yang Lee, Nucl. Phys. **A520**, 641c (1990).
[22] R. Krücken, in *Proceedings of the International Symposium on Advances in Nuclear Physics, Bucharest, Romania, 1999,* edited by D. Poenaru and S. Stoica (World Scientific, Singapore, 2000), p. 336.
[23] R. Krücken, J. Res. Natl. Inst. Stand. Technol. **105**, 53 (2000).
[24] A. Dewald, S. Harissopulos, and P. von Brentano, Z. Phys. A **334**, 163 (1989).
[25] G. Böhm, A. Dewald, P. Petkov, and P. von Brentano, Nucl. Instrum. Methods Phys. Res., Sect. A **329**, 248 (1993).
[26] A. Dewald (private communication); B. H. Saha, diploma thesis, University Köln, 2000 (unpublished).